DISTINGUISHABILITY OF LIQUID ENVIRONMENTS IN THE PRESENCE OF BROWNIAN NOISE

ERNEST GRUNWALD AND COLIN STEEL

Department of Chemistry, Brandeis University, Waltham, Massachusetts 02254, USA

This paper extends previous work on the dynamic averaging of distinct liquid environments by cage exchange to include potential energy fluctuations at the cage centers due to Brownian motions of molecules in the cage walls. After a brief review of the effect of cage exchange on the Schrödinger wave train associated with the electronic ground state of the caged molecule, typical magnitudes and time-scales for the Brownian potential energy fluctuations are estimated. Then a zig-zag model for the resulting noise in the wave trains is developed, and applied to analyze distinguishability in the presence of noisy cage exchange. When distinguishability survives the noise, the distinct caged species are fully fledged environmental isomers. Applications of these concepts are discussed.

INTRODUCTION

Solution chemists use models in which the liquid is treated as a polarizable dielectric continuum, and also models in which it is a collection of discrete molecules. The continuum models include the classic theories of Born, Debye, Onsager and others on ionic solvation, interionic effects and polarization by dipolar molecules.[1-6] The subject molecule exists in a spherical 'cavity' and interacts with a single entity, the surrounding continuum. In physical organic chemistry, the 'cavity' becomes the interior of a liquid 'cage,' but the essential feature, that the complex many-body interactions are reduced to two-body interactions of each molecule with its surrounding cage, is the same. In effect, the cage is part of the molecule, and also, because the cage is inseparable from its molecule, the interaction energy of the cage with its molecule is part of the energy of the molecular species, just as in hydrogen cyanide the C–H bond energy is part of the energy of the HCN species. Thus, while recognizing that molecules in liquids do interact, the cage model fits in with the requirement, implied by the laws of dilute solutions, that molecules in liquids act as independent entities.

The models in which liquids are collections of discrete molecules employ extensive computer-aided sampling to arrive at valid statistical–thermodynamic averages.[7-10] Some models borrow elements from both approaches.[11-16] For instance, Oster and Kirkwood[13] deduced intermolecular structure in water and the alcohols while retaining elements of the continuum approach. In the linear free energy approach of Taft and others[14-16] to the prediction of free energies of solvation, the polarity/polarizability parameter Π^* is essentially a continuum property, similar to Onsager's molar polarization, while the hydrogen bond donating and accepting parameters retain elements of the discrete-molecule approach.

In this paper we shall extend the concept of environmental isomers[17] to include the situation in which the cage is subject to Brownian noise. We shall see that these concepts afford a method of judging at which distance from a given molecule the surrounding fluid may be regarded as a continuum and at which shorter distance the discrete-molecule approach becomes preferable.

PREVIOUS WORK

Our aim[17] has been to obtain criteria for the distinguishability of nominally different liquid environments. Since Schrödinger mechanics is part of general wave mechanics, our rudimentary model is a wave train in which the frequency switches stochastically between two distinct values, ν_a and ν_b. The connection to liquid environments will emerge soon. In Figure 1, the amplitude is constant, the transit times between frequencies are short and the residence times at ν_a and ν_b follow exponential distributions whose means, τ_a and τ_b, are equal. Fourier transformation of long wave trains of this sort yield power spectra in the frequency domain, as shown in Figure 2. These spectra are precise replicas of NMR lines when there is exchange between two
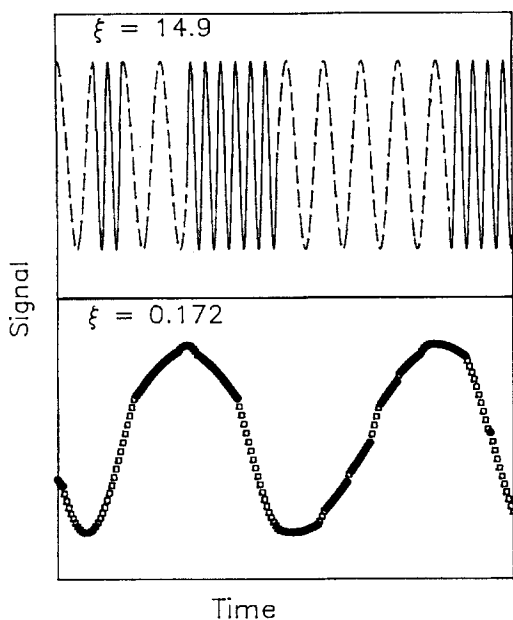
Figure 1. Short sections of the type of wave trains subjected to fast Fourier transformation. As can be seen from Figure 2, the upper train will yield two well resolved lines whereas the lower train, in which switching is more rapid, yields a single collapsed line
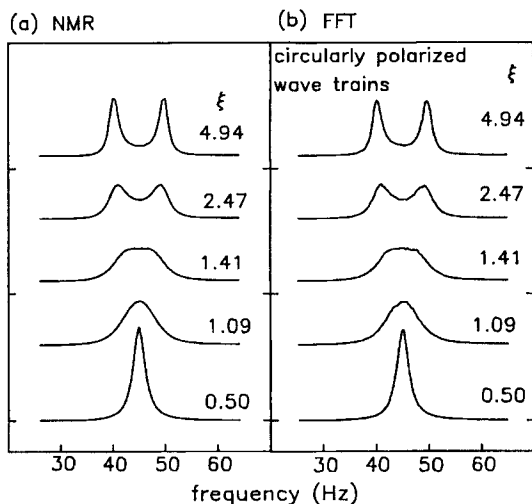

Figure 2. (a) Steady-state solutions of the McConnell–Bloch equations in NMR with v_a and $v_b = 40$ and 50 Hz and $1/T_2 = 0$. (b) Fast Fourier transform power spectra of circularly polarized wave trains with stochastic frequency switching corresponding to exponential lifetime distributions

chemical shifts, as shown by the solutions of the McConnell–Bloch equations[18] plotted alongside the Fourier transforms of the wave trains. In both cases, the line shape depends on a single parameter, the distinguishability index ξ, defined as

$$\xi = 2\pi \,| \, v_a - v_b \, | \, \tau \qquad (1)$$

where $\tau = \tau_a \tau_b / (\tau_a + \tau_b)$. When ξ is large, the spectrum shows separate sharp bands, proving distinguishability. As ξ decreases, these bands first broaden and approach each other. They coalesce when $\xi = \sqrt{2}$, and then collapse into a single sharp line, with loss of distinguishability, as ξ approaches zero.

To establish the connection to Schrödinger waves Ψ, we begin with the stationary-state equation

$$\Psi(x, t) = \phi(x)\exp[-2\pi i(\varepsilon_0/h)t] \qquad (2)$$

where ϕ is the local spatial amplitude and $\exp(-2\pi i[\varepsilon_0/h]t)$ is the time dependence. The latter represents a circularly polarized wave with frequency $v_0 = \varepsilon_0/h$.

It is convenient to let ε_0 denote the energy of the electronic ground state of the isolated molecule, and assume energy additivity for electronic, internal vibrational and other modes. On that basis, the liquid cage effect may be treated as a perturbation of the electronic energy ε_0. This is shown for the simplest case of a one-dimensional cage in Figure 3. The interaction here involves the central molecule (1) and two neighbors, (2) and (3), one on each side. The cage potential is the sum of the pairwise potential energies, with r_{12} increasing to the right and r_{13} to the left. Figure 3(a) shows the symmetric situation when $2 \equiv 3$ so that the (1, 2) and (1, 3) pairwise potentials are identical, and Figure 3(b) depicts the situation when $2 \neq 3$. The two cages thus generate the perturbed electronic energies $\varepsilon_a = \varepsilon_0 + V_a$ and $\varepsilon_b = \varepsilon_0 + V_b$.

Let \a denote the 'a' cage environment and \b the 'b' environment. That is, the central molecule is either (1)\a or (1)\b. As the cage configuration switches between \a and \b, the central molecule exchanges between the subspecies (1)\a and (1)\b, and the electronic ground state energy of (1) switches between ε_a and ε_b. If we identify v_a with ε_a/h and v_b with ε_b/h, the switch in energy is tantamount to a frequency switch. To show that an analogy exists between frequency switching in Schrödinger wave trains and in physical wave trains (such as Figure 1), one must show (i) that the residence times at v_a and v_b are long compared with transit times between v_a and v_b and (ii) that the frequency switching follows the Ehrenfest adiabatic principle,[19] that is, the stationary wave equation (2) applies throughout. As for (i), the central molecule in the cage and any one of its neighbors form an encounter pair whose mean lifetime, as modeled by $\sigma^2/6D$, is of the order 3×10^{-11} s, where σ is the encounter diameter (cage radius) and D is the diffusion coefficient.[20] Since the cage expires when the
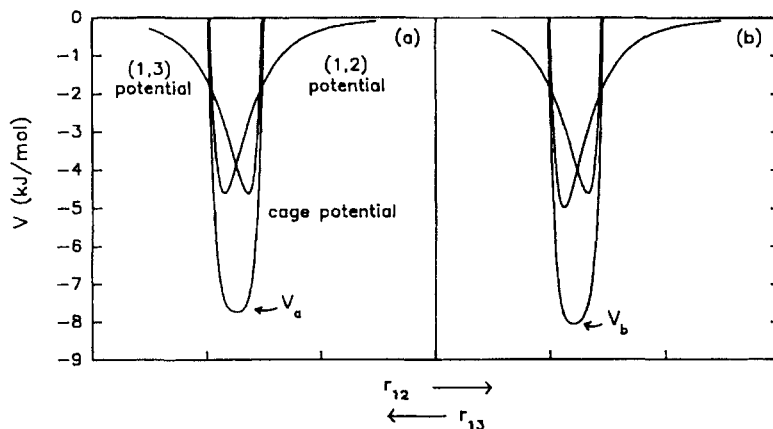
Figure 3. Cage potential for a central molecule (1) with two molecules (2, 3) in its 'solvent' cage. The cage potential is given by $V_{(C)} = V_{(2)}(r_{12}) + V_{(2)}(r_{13})$, where $V_{(2)}$ is the pair potential, and $|r_{12}| + |r_{13}| = d_{(C)}$. For (a) and (b), $d_{(C)} = 12 \cdot 60$ and $12 \cdot 42$ Å, respectively. The pairwise energies are given by $V_{(2)}(r_{ij}) = 4\varepsilon_{LJ(i, j)}[(\sigma_{LJ(i, j)}/r_{ij})^{12} - (\sigma_{LJ(i, j)})/r_{ij})^{6}]$. For cage (a) $\sigma_{LJ(1, 2)} = \sigma_{LJ(1, 3)} = 5.15$ Å, $\varepsilon_{LJ(1, 2)} = \varepsilon_{LJ(1, 3)} = 4 \cdot 63$ kJ mol^{-1}. For cage (b) $\sigma_{LJ(1, 3)}$ and $\varepsilon_{LJ(1, 3)}$ are as for (a) and $\sigma_{LJ(1, 2)} = 5 \cdot 0$ Å and $\varepsilon_{LJ(1, 2)} = 5 \cdot 0$ kJ mol^{-1}

encounter pair breaks up, 3×10^{-11} s is also the order of the cage lifetime (τ). On the other hand, the transit time between the \a and \b states is of order 10^{-13} s, the time-scale of atomic displacements or vibrations. Thus condition (i) is satisfied. As for (ii), even the shorter of the time-scales in (i) is long compared with the 10^{-15} s time-scale for electronic motions, so that condition (ii) is also satisfied. We may conclude, therefore, that the Schrödinger wave of the electronic ground state of a cage-switching molecule in a liquid shows exchange averaging just like the physical waves in Figure 1. The line shape depends on the value of ξ. Equation (1) is transformed to equation (3) by letting $\nu = E/hN_A$:

$$\xi = 2\pi |E_a - E_b| \frac{\tau}{hN_A} \quad (3)$$

where E denotes energy per mole and N_A is Avogadro's number. When E is given in J mol^{-1} and τ in s, equation (3) becomes $\xi = 1 \cdot 575 \times 10^{10} |E_a - E_b| \tau$. In applying equation (3), we shall use the convention that two cage environments are clearly distinguishable when $\xi \geqslant 5$, and are exchange averaged when $\xi \leqslant 1$. In the intermediate range the distinguishability is borderline.

SOME REPRESENTATIVE NUMBERS

On introducing 3×10^{-11} s for τ and $\geqslant 5$ for ξ, equation (3) states that distinguishability exists when $|E_a - E_b| \geqslant 10$ J mol^{-1}. Compared with absolute solvation energies, 10 J mol^{-1} is small, but Figure 3 shows, schematically, that the differences between solvation energies might be expected to be small.

To obtain quasi-empirical estimates, we shall use Hildebrand's regular-solution model[21] to predict

$\Delta_{benz}E_{a,b}$ for the process benzene\a $\rightarrow$ benzene\b. Here \a is a cage consisting of all-benzene neighbors and \b is a cage consisting of one B neighbor and the rest benzene neighbors. The calculation consists of two steps. (i) The energy of transfer per mole of benzene from pure benzene to a dilute solution of benzene in liquid B is $\Delta E_B = V_{benz}(\delta_B - \delta_{benz})^2$, where V is the molar volume and δ is Hildebrand's solubility parameter, $\delta = (\Delta E_{vap}/V)^{1/2}$. (ii) In step (i), a benzene molecule transfers from an all-benzene environment to an all-B environment. If the benzene molecule has s B neighbors in the latter, then the energy $\Delta_{benz}E_{a,b}$ for introducing one B neighbor is of the order of $\Delta E_B/s$. In the following, we shall use $s = 10$.

Results for some 'regular' neighbors are given in Table 1. One out of the 12 cases is exchange-averaged, one case is marginal and all others are distinguishable.

In ideal solutions, heats of mixing are zero by hypothesis and environmental isomerism is out.[21] In regular solutions, heats of mixing are far from large, yet the above discussion indicates that environmental isomerism should be fairly common. However, this isomerism is generally masked because of the potential energy fluctuations arising from Brownian motion of molecules in the cage wall, and it is this problem that we now address.

Amplitude of potential energy noise

We shall use two model liquids: (a) idealized benzene, i.e. benzene with a spherically symmetrical cage potential based on Lennard–Jones 6–12 pairwise potentials whose parameters reproduce the properties of dilute benzene gas; (b) idealized water, i.e. water with a cage potential based on Lennard–Jones pairwise interactions

Table 1. Estimates of $\Delta_{benz}E_{a,b}$ based on Hildebrand's solubility parameters and the regular-solution model[a]

B	δ	$\Delta_{benz}E_{a,b}$	ξ^a	Comment[b]
CCl$_4$	17·6	13	6	D
(CH$_3$)$_4$Si	12·7	330	160	D
CH$_2$I$_2$	24·1	250	120	D
Cl$_2$C=CCl$_2$	19·0	0·4	0·2	A
CS$_2$	20·5	26	12	D
(C$_4$F$_9$)$_3$N	12·1	400	190	D
(C$_2$H$_5$)$_2$O	15·1	120	60	D
n-Hexane	14·9	140	60	D
Cyclohexane	16·6	43	20	D
C$_6$F$_{14}$	12·1	400	190	D
Toluene	18·2	3	1·5	M
Naphthalene	20·3	20	10	D

[a] Ref. 21. Energy values in J mol^{-1}. δ Values in J$^{1/2}$ cm$^{-3/2}$. $V_{benz} = 89$ cm^3 mol^{-1}; $\delta_{benz} = 18\cdot8$; $\tau = 3 \times 10^{-11}$ s; $s = 10$; $\xi = 0\cdot47\Delta_{benz}E_{a,b}$.
[b] A = exchange-averaged; D = distinguishable; M = marginal.

to which has been added a molecule dipole–cage dipole interaction inferred from the dielectric constant.[22] The cages will be spherical, and the molecules are moving independently. The noise is measured by $\sigma_{(C)}$, the standard deviation of the fluctuating cage potential at the cage center.

(a) The primary molecule is treated as stationary at the cage center. The first step is to obtain the mean amplitude of libration of one of the cage molecules in its own cage (Figure 4). The libration is in all possible directions, but only the motion along the line of centers to the substrate molecule is relevant to our calculation. We first find q_{RT}, the amplitude of libration normal to the cage wall when the mechanical energy (potential + kinetic) equals the mean thermal energy RT. We then calculate the variance, $\sigma_{(2)}^2$, in the pair potential $V_{(2)}$ due to the Brownian motion between $+q_{RT}$ and $-q_{RT}$.
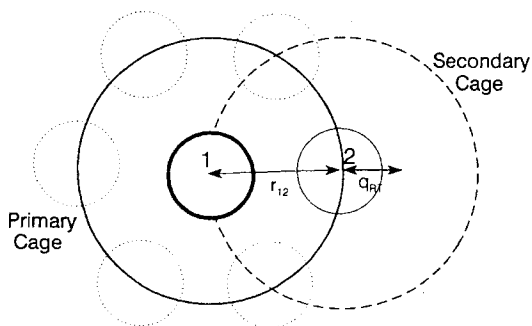

Figure 4. Molecule 1 surrounded by its cage, which is shown as a full circle. The cage of one of the molecules (2) comprising the cage wall of 1 is shown as the dashed circle. Brownian motion of 2 in its cage affects the potential of 1 through the varying 1,2-pairwise interaction.

Finally, we calculate $\sigma_{(C)}^2 = s\sigma_{(2)}^2$, the variance in the potential of the primary molecule at its cage center, where s is the number of neighbors in the cage wall. Since the overall noise results from the convolution of s independent pairwise noise distributions, the shape of the overall distribution is nearly Gaussian, regardless of the shapes of the pairwise distributions. The near-Gaussian shape follows from the central limit theorem.[23] The theorem predicts a strictly Gaussian shape in the limit as s goes to infinity. In practice, Gaussian-like envelopes are produced when s is as small as 5.[23]

For benzene the Lennard–Jones parameters are $\varepsilon_{LJ} = 4\cdot63$ kJ mol^{-1} and $\sigma_{LJ} = 5\cdot15$ Å.[24] For $s = 10$ these parameters yield $q_{RT} = 0\cdot87$ Å and the standard deviation of the fluctuating cage potential $\sigma_{(C)} = 2\cdot6$ kJ mol^{-1} (kilojoules, not joules!).

(b) In the two-state model of water, one state has $s = 4$, the other $s = 5$.[22] In the model used, the dipole axis of the caged water molecule defines the z-axis of the Cartesian coordinate system. The s water molecules in the cage wall are placed so that $s/6$ interact with the central water molecule from any of the six Cartesian directions. Thus, from any direction, we have $s/6$ Lennard–Jones pairwise interactions with $\varepsilon_{LJ} = 6\cdot0$ kJ mol^{-1} and $\sigma_{LJ} = 2\cdot72$ Å. In the z-direction we have an additional water dipole–cage interaction, given[22] for $s = 4$ by $V_{dd} = -240\cdot7/(3\cdot15 + q_z)^3 - 240\cdot7/(3\cdot15 - q_z)^3$ kJ mol^{-1}, where q_z is in Å. For $s = 5$ the expression becomes[22] $V_{dd} = -109\cdot0/(3\cdot15 + q_z)^3 - 109\cdot0/(3\cdot15 - q_z)^3$.

For $s = 4$, $q_{RT} = 0\cdot18$ Å and $\sigma_{(C)} = 1\cdot24$ kJ mol^{-1} along z, and $q_{RT} = 0\cdot28$ Å and $\sigma_{(C)} = 0\cdot90$ kJ mol^{-1} along x and y. For $s = 5$, the corresponding mean values are $0\cdot26$ Å and $0\cdot97$ kJ mol^{-1}. In the following we shall actually use the values of $q_{RT} = 0\cdot25$ Å and $\sigma_{(C)} = 1\cdot05$ kJ mol^{-1} for both the s-states.

SCHRÖDINGER WAVE TRAINS WITH BROWNIAN FREQUENCY NOISE

According to our calculations (Table 1), cage-energy differences $|E_b - E_a|$ in regular solutions tend to be small compared with the standard deviations $\sigma_{(C)}$ of the noise in the cage potential. As a result, we must deal with issues that are not part of the daily ration of a solution chemist: (i) the time-scale and possible exchange-averaging of the fluctuations, (ii) the impact (if any) on the validity of the Ehrenfest adiabatic principle and (iii) distinguishability in the presence of noise. These issues will now be considered. As a first step, we shall propose a suitable model for the Brownian fluctuations.

Zig-zag model

A Schrödinger wave whose potential energy fluctuates about a mean value ε_1 with a standard deviation $\sigma_{(C)}$

mimics an FM wave whose carrier frequency v_1 equals ε_1/h, and whose frequency modulation is random frequency noise with a standard deviation of $\sigma_{(C)}/h$. As discussed above, the distribution function for the potential energy (and hence for the random modulation frequencies) is virtually Gaussian. Figure 5 shows a short segment of a wave train with a single carrier frequency v_1 and (exaggerated) frequency modulation. We are assuming here that the frequency follows the zig-zag model for Brownian frequency noise pictured in Figure 6. This model is inspired by the fact that the Brownian paths of micron-size particles suspended in liquids, when observed under a microscope, appear to be zig-zags. Apparently, most of the time the net force from the environment is relatively ineffective, but occasionally a force lies far out in a wing of a distribution function and then is strong enough to kick the particle towards a random new position in the Gaussian frequency distribution. A reader familiar with gas-phase kinetics will recognize that the zig-zag model is the Brownian analog of the strong-collision model of kinetic theory.[25] Note that the noise generated in Figure 6 has the typical spiky appearance of real noise. The mean time between the sharp changes of slope is identified with the Brownian correlation time, which will now be discussed.

Correlation time

The time-scale for noisy fluctuations is given by the correlation time τ_{corr}.[26] For random noise due to Brownian motion we may think of τ_{corr} as a dynamical memory time. In the absence of Brownian forces the dynamic
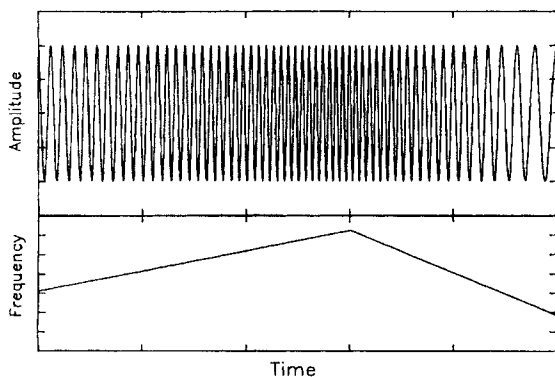

Figure 5. A short segment of a wave train in which the frequency varies based on the zig-zag model of Brownian frequency modulation. The observation time is of order $2\tau_{corr}$, where τ_{corr} is the mean of the individual correlation times (t_i). The frequency first increases linearly for t_i, then changes to a new rate for t_{i+1}, both chosen stochastically. The modulation is exaggerated; on a realistic scale the modulation would be nearly invisible
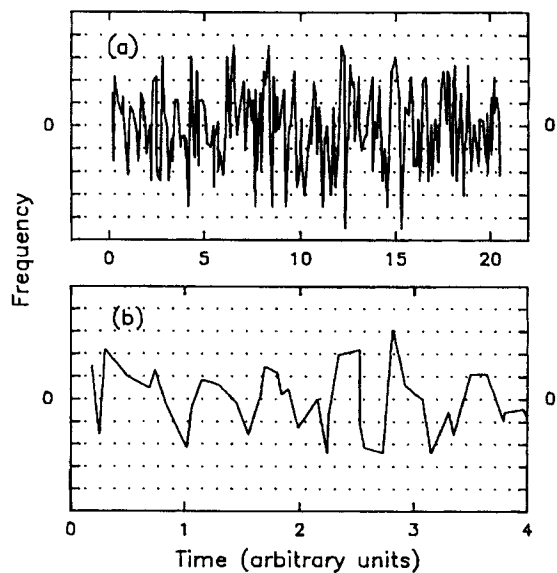

Figure 6. Zig-zag model of Brownian frequency noise. (a) Plot of v vs time for about $100\tau_{corr}$. (b) A segment of (a) expanded by a factor of 5

path of a molecule can be predicted from the boundary conditions at $t = 0$, but the continual Brownian barrage induces statistical deviations from the predicted path and, after a mean time τ_{corr}, destroys its memory. The mean time between the sharp changes of slope equals τ_{corr}, while the individual times follow an exponential distribution about this mean.

To obtain numerical values for τ_{corr} for potential-energy fluctuations in a liquid cage, we shall refer to chemical kinetics. According to the principle of dynamic balance, the rate laws and rate constants for the forward and reverse reactions in a kinetic system on its way to equilibrium remain valid at dynamic equilibrium. This principle has been well tested, by comparing rates of relaxation to equilibrium with rates of exchange *at* equilibrium.[27] In the statistical theory of Brownian motion, the fluctuation-dissipation theorem plays an analogous role,[26] by connecting the relaxation of Brownian ensembles *to* equilibrium with the turnover dynamics *at* equilibrium. For example, rate constants for dielectric relaxation to rotational equilibrium in liquids may be identified with $1/\tau_{corr}$ for the redistribution of molecules among the rotational energy values at equilibrium.[28]

In the present case, the Fokker–Planck equation has been solved[26] for the relaxation to equilibrium of Brownian ensembles in quadratic potential wells of the form, $V = RT(q/q_{RT})^2$. The relaxation time for the ensemble average of q^2, $\langle q^2 \rangle$, and hence for $\langle V \rangle$, is given by $q_{RT}^2/4D$, where D is the coefficient of linear diffusion for the given liquid.[26] Although the potential

wells in our problem are not strictly quadratic, the model is close enough. We shall therefore evaluate τ_{corr} via the equation

$$\tau_{corr} = q_{RT}^2/4D \qquad (4)$$

For benzene at 298 K, $D = 2 \cdot 3 \times 10^{-5}$ cm^2 s^{-1},[29] and $q_{RT} \approx 8 \cdot 7 \times 10^{-9}$ cm (see above), hence $\tau_{corr} \approx 8 \times 10^{-13}$ s. For water at 298 K, $D = 2 \cdot 25 \times 10^{-5}$ cm^2 s^{-1},[30] and $q_{RT} \approx 2 \cdot 5 \times 10^{-9}$ cm, hence $\tau_{corr} \approx 0 \cdot 7 \times 10^{-13}$ s. Note that the order of $1/\tau_{corr}$ (10^{12}–10^{13} s^{-1}) agrees with that of the hard-sphere collision frequency per molecule predicted for common liquids.

For our purpose, the key point is that τ_{corr} is long enough for the Ehrenfest adiabatic principle to hold. That is, the electronic ground state of the caged molecule is a stationary state, although its energy is noise-broadened. We also learn that τ_{corr} is about 100 times shorter than the cage-exchange time τ. This implies a barrier of order $RT \ln(100)$ between the cages.

Noisy wave train

As is well known to users of Fourier transform spectrometers, data in the time domain and their transforms in the frequency domain express the same reality. For wave trains it is natural to start in the time domain, but when the wave incorporates stochastic frequency fluctuations it is convenient to transform to the frequency domain, for the infinity of fluctuations then becomes compressed into a single power spectrum which can be understood at a glance. We shall begin, therefore, with Schrödinger wave trains in the time domain and end up with their power spectra.

In this section we examine the effect of the Brownian correlation time on the spectral band width. There is some kinship between this and the natural 'line' width

in magnetic resonance spectra, except of course that our width relates to an electronic ground state rather than to a spectral transition. As is well known, natural line widths in magnetic resonance[31] are fairly sensitive to τ_{corr}, and we might expect some sensitivity here because potential-energy fluctuations themselves are a kind of exchange process prone to exchange averaging.

In our computer simulations we used the zig-zag model for Brownian frequency noise, and parameters corresponding to $\varepsilon_0 = -40$ kJ mol^{-1}, $\sigma_{(C)} = 1 \cdot 0$ kJ mol^{-1} and τ_{corr} either $0 \cdot 7 \times 10^{-13}$ s (as for water) or 8×10^{-13} s (as for benzene). The resulting Fourier transforms are shown in Figure 7. The shorter τ_{corr} produces the narrower band, but the two half-widths are within a factor of two even though τ_{corr} varies by more than tenfold, and the broader width is just less than $\sigma_{(C)}$. We conclude that in contrast to NMR, in the present problem the band widths are rather insensitive to τ_{corr}.

Inclusion of cage exchange

In Figure 6 we considered wave trains with Brownian frequency modulation and a single carrier frequency. In Figure 8 we consider similarly noisy wave trains in which the carrier frequency switches stochastically between two frequencies, ν_a and ν_b, characteristic of two discrete cages. Each line shows one cycle of exchange ($\backslash$a $\rightarrow$ $\backslash$b $\rightarrow$ $\backslash$a), with the $\backslash$b segment always occurring in the middle half. Magnitudes of the ratio $\zeta = (E_b - E_a)/\sigma_{(C)}$ vary from $0 \cdot 35$ to $5 \cdot 0$. The dissonance of the Brownian frequency noise tends to obscure the switching points. Cage switching is clear when $\zeta = 5 \cdot 0$, marginally visible when $\zeta = 2 \cdot 0$ and essentially invisible when $\zeta \leqslant 1 \cdot 5$. The mean cage exchange time τ in these plots is about 40 times longer than τ_{corr}.
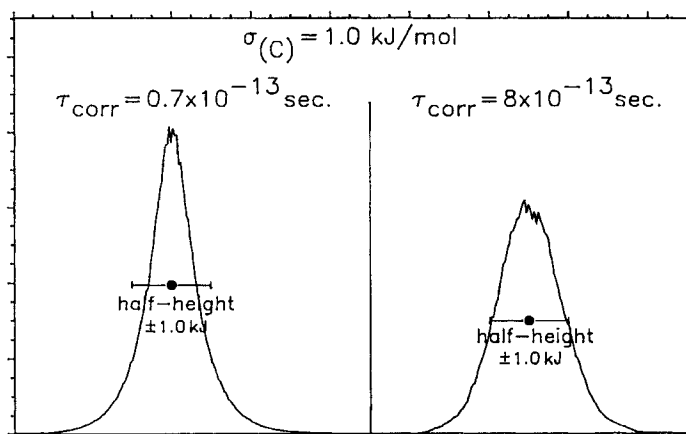

Figure 7. Effect of the correlation time for the Brownian noise on the band width in the frequency domain. Noisy wave trains in the time domain were simulated using the zig-zag model described in the text
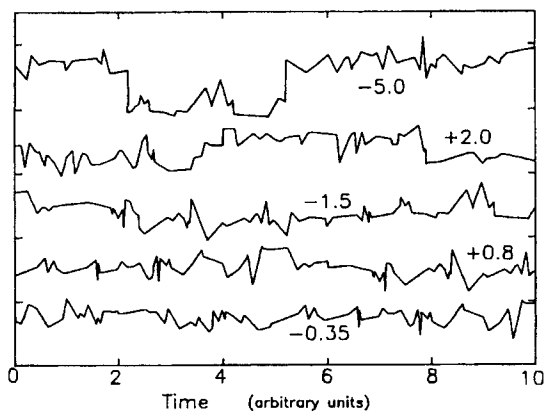
Figure 8. Brownian frequency noise with cage exchange. Each segment is labelled by its value of ζ [$= |E_b - E_a|/\sigma_{(C)}$], and shows one cycle of exchange (\a $\rightarrow$ \b $\rightarrow$ \a) with the b section always occurring in the middle half. Only when $|\zeta| \gtrsim 5$ is exchange clear; otherwise it is masked by noise

Power spectra resulting from Fourier transforms of long, noisy, frequency-switching wave trains are clearer, as shown in Figures 9 and 10. Values of ξ [equation (3)] are 40 throughout, so that in the absence of Brownian noise each power spectrum would consist of two narrow bands, suggested by the 'sticks' in the figures. The parameters adopted in Figure 9 are intended to resemble those for benzene at room temperature. The figure assumes equal cage populations. The smallest

value of $|E_b - E_a|$, 0.9 kJ mol^{-1} [$0.35\sigma_{(C)}$], was chosen as a real possibility for benzene because it fits the predicted energy difference for the two lowest pairwise potential minima.[32] The power spectrum here is a symmetrical band whose \a : \b components overlap so strongly that practical distinguishability is out. The other values for $|E_b - E_a|$ exceed realistic possibilities and are purely instructive. There are two recognizable peaks in both. These peaks coalesce (not shown) when $|E_b - E_a| \approx 1.5\sigma_{(C)}$.

The parameters adopted in Figure 10, including the relative cage populations of $0.7/0.3$ and $|E_b - E_a| = 10$ kJ mol^{-1}, as shown in (d), are intended to fit the two-state model for water.[22] The smaller values for $|E_b - E_a|$ are instructive only. Distinguishability is strong when $|E_b - E_a| = 10$ kJ mol^{-1} [$9.5\sigma_{(C)}$], and it is clear that the two states of water could easily be environmental isomers. Distinguishability in the form of distinct peaks or a shoulder persists down to $|E_b - E_a| \approx 1$ kJ mol^{-1} ($1\sigma_{(C)}$, not shown). When $|E_b - E_a| = 0.35\sigma_{(C)}$, the peaks overlap so strongly that a single, seemingly symmetrical band results.

As $\zeta = |E_b - E_a|/\sigma_{(C)}$ decreases, it is tempting to identify the loss of distinguishability with coalescence of the separate bands in the power spectrum, which (depending on τ/τ_{corr} and relative peak height) occurs in the range $1 < \zeta < 2$. Considerations based on information theory (not described here) indicate, however, that this criterion is conservative, and that with careful design, ζ might be reduced to nearly half of the preceding estimate.
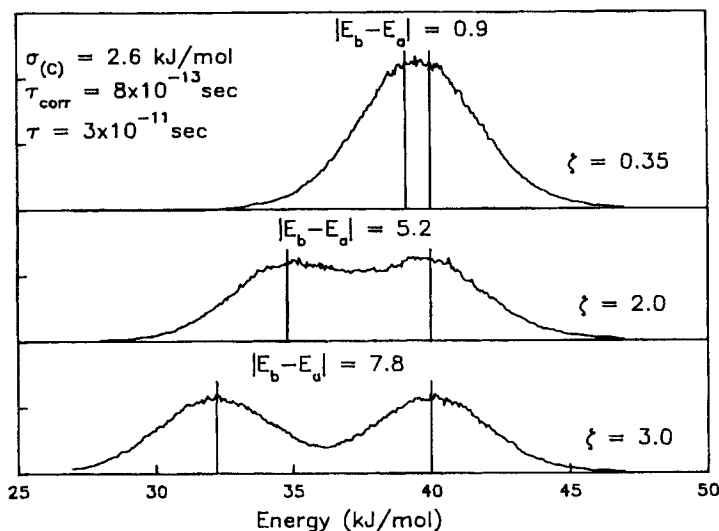

Figure 9. Model power spectra for liquids having benzene-like values for $\sigma_{(C)}$, τ_{corr} and τ. Units for $|E_b - E_a|$ are kJ mol^{-1}. When $|E_b - E_a| = 0.9$ kJ mol^{-1}, $\xi \approx 400$
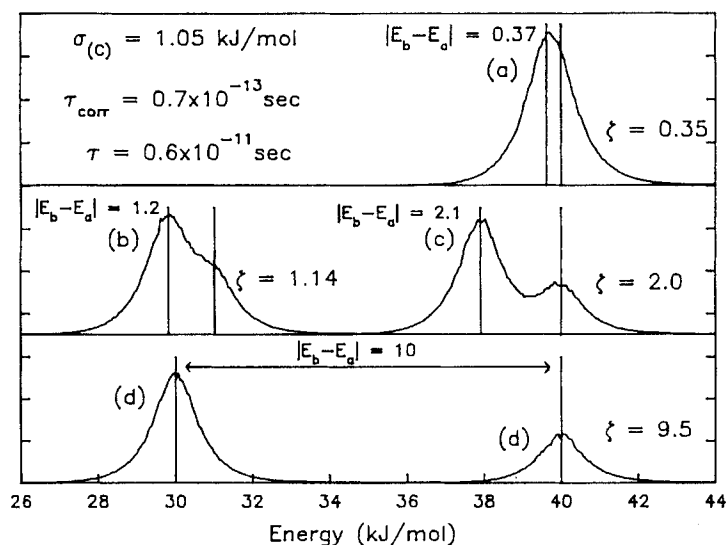
Figure 10. Model power spectra for liquids having water-like values for $\sigma_{(C)}$, τ_{corr} and τ. Units for $|E_b - E_a|$ are kJ mol^{-1}. The cage populations are in the ratio 0.7/0.3. When $|E_b - E_a| = 10.0$ kJ mol^{-1}, $\xi \approx 1000$

DISCUSSION

Chemists usually deal with the spatial part of the Schrödinger wave function, on the assumption that the system is in a stationary state. This may not be true however, because real-life systems are subject to external perturbations. Retaining the time-dependent part of the wave function then gives a more complete picture of the system. Of course, in spectroscopy we only observe the Schrödinger wave indirectly, since the spectral frequency equals the difference between the frequencies of the Schrödinger waves associated with the initial and final states in the transition. However, this does not lessen the importance of the underlying state wave functions, neither the spatial nor the time dependent parts.

One prediction which emerges clearly from the present work is that there are two kinds of distinguishability in liquids, which will be called 'ideal' and 'real.' Ideal distinguishability is based on cage exchange in the absence of Brownian potential energy noise and only requires the absence of cage-exchange averaging. As a corollary, the distinguishability index ξ, defined in equation (3), must be $>x$, where x is of the order of 1–5.

Real distinguishability requires not only the absence of cage-exchange averaging, but also that the cage-energy difference $|E_b - E_a|$ be sufficiently great to stand out over the Brownian noise so that $\zeta = |E_b - E_a|/\sigma_{(C)} \geqslant y$, where y is of the order of 1–2. This is practical or operational distinguishability, so that the molecules occupying the different cages are genuine

isomers (environmental isomers) by orthodox chemical standards. As stated in previous papers,[17] a likely example are the two 'states' of liquid water. The two-state model for water has had trouble being accepted, in spite of good experimental evidence,[33] because without environmental isomers the nature of the two states is hard to rationalize. The HOH molecule has just one stable structure, not two. Also, if hydrogen-bonded complexes were forming, one would expect to find numerous complexes, not two. On the other hand, Figure 10 shows that the two states of water would be distinguishable if they were environmental isomers. Evidence concerning the nature of two water cages was discussed by Grunwald[22] some years ago, and Benson and Siebert[34] have shown how the thermodynamics of water can most readily be understood in terms of a two-state model. Further, as will be shown in a future paper,[35] the concept of environmental isomers provides a simple explanation for the remarkable enthalpy–entropy compensation that has been observed in certain association equilibria.[36]

The above discussion has been in terms of a molecule and its first solvation shell (primary cage) (Figure 4). There will also be a second shell at a greater distance. Since pairwise interaction energies vary strongly with distance, approximately as $1/r^6$, a change in the configuration of the second shell will result in a much smaller value for $|E_a - E_b|$ compared with the value for the first shell, roughly $1/64$ [$= (1/2)^6$]. In terms of equation (3) and typical values such as are given in Table 1, this indicates that beyond the second shell $\xi \leqslant 1$, and here exchange averaging will be the norm. At

such distances the liquid becomes a genuine continuum. For example, the ion clouds visualized by the Debye–Hückel theory[2] as forming around ions in highly dilute solutions may now be seen to be genuine continua. It is interesting that such distances correspond to the distance at which structure associated with the pair distribution function becomes strongly damped.[10]

In between there are regions of borderline distinguishability, both real and ideal. Onsager's theory of the dielectric constant[3] has the caged polarizable dipole interact with a polarizable dielectric continuum. The liquids treated successfully in this way tend to fit regular-solution models and, judging by Table 1, ideal distinguishability mostly exists. On the other hand, the magnitudes of $\zeta = |E_b - E_a|/\sigma_{(C)}$ are well below unity, and real distinguishability is mostly out. We infer, therefore, that for dielectric purposes, low values of ζ, even though coupled with ideal distinguishability ($\xi > 1$), may be sufficient to produce continua.

ACKNOWLEDGMENT

REFERENCES

1. M. Born, Z. Phys. 1, 45 (1920).
2. P. Debye and E. Hückel, Phys. Z. 24, 185 (1923).
3. L. Onsager, J. Am. Chem. Soc. 58, 1486 (1936).
4. H. L. Friedman, J. Chem. Phys. 76, 1092 (1982).
5. (a) F. J. O. del Valle and J. Tomasi, Chem. Phys. 150, 138 (1991); (b) M. A. Aguilar, F. J. O. del Valle and J. Tomasi, Chem. Phys. 150, 151 (1991).
6. (a) A. A. Rashin and B. Honig, J. Phys. Chem. 89, 5588 (1985); (b) E. Grunwald, G. Baughman and G. Kohnstam, J. Am. Chem. Soc. 82, 5801 (1960).
7. F. H. Stillinger and A. Rahman, J. Chem. Phys. 57, 1281 (1972).
8. W. L. Jorgensen, J. Phys. Chem. 87, 5304 (1983).
9. G. Ciccotti and W. G. Hoover (Eds), Molecular Dynamics Simulation of Statistical Mechanical Systems (ASI–NATO Course). North-Holland, Amsterdam (1986).
10. F. Hirata, P. J. Rossky and B. M. Pettit, J. Chem. Phys. 78, 4133 (1983).
11. C. J. Cramer and D. J. Truhlar, J. Am. Chem. Soc. 113, 8305 (1991).
12. W. C. Still, A. Tempczyk, R. C. Hawley and T. Hendrickson, J. Am. Chem. Soc. 112, 6127 (1990).
13. G. Oster and J. G. Kirkwood, J. Chem. Phys. 11, 175 (1943).
14. (a) M. J. Kamlet and R. W. Taft, J. Am. Chem. Soc. 98, 377 (1976); (b) R. W. Taft and M. J. Kamlet, J. Am. Chem. Soc. 98, 2886 (1976); (c) T. Yokoyama, R. W. Taft and M. J. Kamlet, J. Am. Chem. Soc. 98, 3233 (1976).
15. J. L. M. Abboud, M. J. Kamlet and R. W. Taft, Prog. Phys. Org. Chem. 13, 485 (1981).
16. M. H. Abraham, Chem. Soc. Rev. 22, 73 (1993).
17. (a) E. Grunwald and C. Steel, J. Phys. Chem. 97, 13326 (1993); (b) E. Grunwald and C. Steel, Pure Appl. Chem. 65, 2543 (1993).
18. H. M. McConnell, J. Chem. Phys. 28, 430 (1958).
19. R. C. Tolman, The Principles of Statistical Mechanics, p. 414. Oxford University Press, London (1938).
20. M. Eigen, Z. Phys. Chem. (N.F.) 1, 176 (1954).
21. J. H. Hildebrand and R. L. Scott, Regular Solutions, Chapt. 7, pp. 90–91. Prentice-Hall, Englewood Cliffs, NJ (1962).
22. E. Grunwald, J. Am. Chem. Soc. 108, 5719 (1986).
23. R. N. Bracewell, The Fourier Transform and Its Applications, 2nd edn. McGraw-Hill, New York (1978).
24. D. Ben-Amotz and D. R. Herschbach, J. Phys. Chem. 94, 1038 (1990).
25. R. G. Gilbert and S. C. Smith, Theory of Unimolecular and Recombination Reactions, p. 246. Blackwell, Oxford (1990).
26. R. K. Pathria, Statistical Mechanics, p. 462. Pergamon Press, New York (1972).
27. E. Grunwald, Prog. Phys. Org. Chem. 3, 317 (1965).
28. P. Debye, Polar Molecules, Chapt. 5. Dover, New York (1945).
29. H. J. Parkhurst and J. Jonas, J. Chem. Phys. 63, 2698 (1975).
30. E. O. Stejskal and J. E. Tanner, J. Chem. Phys. 42, 288 (1965).
31. J. A. Pople, W. G. Schneider and H. J. Bernstein, High-Resolution Nuclear Magnetic Resonance, Chapt. 9. McGraw-Hill, New York (1959).
32. W. L. Jorgensen and D. L. Severance, J. Am. Chem. Soc. 112, 4768 (1990).
33. (a) G. E. Walrafen, M. S. Hokmabadi, M. R. Fischer and W.-H. Yang, J. Chem. Phys. 85, 6970 (1986); (b) J. D. Worley and I. M. Klotz, J. Chem. Phys. 45, 2868 (1966).
34. S. W. Benson and E. D. Siebert, J. Am. Chem. Soc. 114, 4269 (1992).
35. E. Grunwald and C. Steel, in preparation.
36. A. F. Danil de Namor, M.-C. Ritt, M.-J. Schwing-Weill, F. Arnaud-Neu and D. F. Lewis, J. Chem. Soc., Faraday Trans. 3231 (1991).